

# Impact of Human Adenovirus Type 3 Dodecahedron on Host Cells and Its Potential Role in Viral Infection

Pascal Fender,<sup>a</sup> Kathryn Hall,<sup>b</sup> Guy Schoehn,<sup>a</sup> and G. Eric Blair<sup>b</sup>

CNRS, Unit of Virus Host Cell Interaction, Grenoble, France,<sup>a</sup> and Institute of Molecular and Cellular Biology, Faculty of Biological Sciences, University of Leeds, Leeds, United Kingdom<sup>b</sup>

**During human adenovirus type 3 (Ad3) infection, an excess of penton base and fiber proteins are produced which form dodecahedral particles composed of 12 pentamers of penton base and 12 trimers of fiber protein. No biological functions have yet been ascribed to Ad3 dodecahedra. Here, we show that dodecahedra compete with Ad3 virions for binding to the cell surface and trigger cell remodeling, giving new insights into possible biological functions of dodecahedra in the Ad3 infectious cycle.**

Human adenoviruses (Ads) are nonenveloped viruses which cause a variety of respiratory, ocular, and enteric infections. The capsid is composed of three major proteins: hexon, penton base, and fiber. Hexon trimers form the facets of the icosahedron, with pentamers of penton base located at each of the capsid vertices, from which projects a trimeric fiber protein. The noncovalent complex of pentameric base and trimeric fiber is referred to as the penton and mediates attachment and entry of the virus. Adenoviruses from all six human species use the coxsackievirus and adenovirus receptor (CAR) as their primary site of attachment, with the exception of species B viruses (7). Recently, desmoglein-2 (DSG-2) was identified as an attachment molecule for certain species B Ads, including serotypes 3, 7, 11, and 14 (13). During the replication cycle of these serotypes, an excess of a symmetrical complex comprising 12 pentons is formed, termed the penton-dodecahedron (Pt-Dd) (2, 3, 8, 11). No function has yet been assigned to this unique particle. Using human adenovirus type 3 (Ad3), we show here that Pt-Dd competes with virions for attachment to the cell surface, internalizes DSG-2, and triggers remodeling of cell morphology, suggesting a possible role for this complex during Ad infection.

To monitor Pt-Dd distribution during Ad3 infection, HeLa cells were infected with 0.1 PFU/cell of wild-type Ad3. At 24, 48, and 72 h postinfection (hpi), cells were fixed and permeabilized and Pt-Dd and DSG-2 were localized by immunofluorescence. As expected, Pt-Dd colocalized with infected cells (indicated by the stars in Fig. 1A) but was also detected by anti-fiber antibody in the surrounding uninfected cells at 48 and 72 hpi (Fig. 1A). In addition, Pt-Dd was found along with DSG-2 at the contact between two cells (Fig. 1A, highlighted in the white box at 48 hpi). Pt-Dd was also found in uninfected cells using a separate antibody raised against Pt-Dd (4). The white arrows in Fig. 1B indicate Pt-Dd staining in surrounding uninfected cells and also the Pt-Dd signal along the interface between two cells. Since both the anti-fiber and anti-Pt-Dd antibodies can bind to whole virus as well as to Pt-Dd, the possibility that the cytoplasmic staining observed in uninfected cells was due to Ad3 was excluded by the presence of detectable hexon only in nuclei of Ad3-infected cells (see Fig. S1 in the supplemental material). These findings suggest that Pt-Dd is released from infected cells, prior to the release of progeny virus, and can bind to the periphery of neighboring cells via DSG-2.

To determine whether Pt-Dd competes with Ad3 for binding to the cell surface, competition assays were performed. As a con-

trol, the effect of base-dodecahedron (Bs-Dd) (which consists of only Ad3 penton base but no fiber proteins) on Ad3 attachment was also assessed. The integrity of these protein complexes was confirmed by transmission electron microscopy (see Fig. S2 in the supplemental material). Increasing concentrations of either Bs-Dd or Pt-Dd were incubated at room temperature with A549 cell monolayers for 30 min prior to the addition of Ad3 virus expressing enhanced green fluorescent protein (Ad3-EGFP) (9). Pretreatment of A549 cells with Pt-Dd led to a reduction in Ad3-mediated EGFP expression in a dose-dependent manner; however, Bs-Dd did not inhibit Ad3-EGFP entry (Fig. 2A). In a complementary approach, A549 cells were preincubated with Pt-Dd at 37°C for 2 h in order to internalize cell surface attachment molecules prior to the addition of Ad3-EGFP. This resulted in a comparable effect, namely, a reduction in EGFP expression following Pt-Dd, but not Bs-Dd, pretreatment (Fig. 2B). This suggested that the cell surface molecule bound by Pt-Dd and also used by Ad3-EGFP for attachment was internalized by Pt-Dd. This was confirmed by colocalization of internalized DSG-2 with Pt-Dd in A549 cells (Fig. 2C). Pt-Dd also blocked Ad3-EGFP entry into primary human endothelial cells, suggesting that this was a physiological effect and was not confined to cancer cells such as A549 or HeLa cells (Fig. 2D). Overall, these results show that Pt-Dd competes with Ad3 virions by both occupying cell surface attachment molecules and triggering their internalization.

As Pt-Dd is released from Ad3-infected cells and can bind to DSG-2 on the surface of adjacent cells, the potential effects of this complex on uninfected cells were analyzed. Cells were incubated at 37°C with either Cy5-labeled Bs-Dd (Cy5-Bs-Dd) or Pt-Dd (Cy5-Pt-Dd), fixed, permeabilized, and incubated with rhodamine-labeled phalloidin to label actin microfilaments. Untreated control cells remained as a uniform monolayer with cortical actin staining (Fig. 3A, Ctl). However, incubation with Pt-Dd for 60

Received 16 December 2011 Accepted 7 February 2012

Published ahead of print 15 February 2012

Address correspondence to Pascal Fender, pfender@embl.fr.

P.F. and K.H. contributed equally to this article.

Supplemental material for this article may be found at <http://jvi.asm.org/>.

Copyright © 2012, American Society for Microbiology. All Rights Reserved.

doi:10.1128/JVI.07127-11

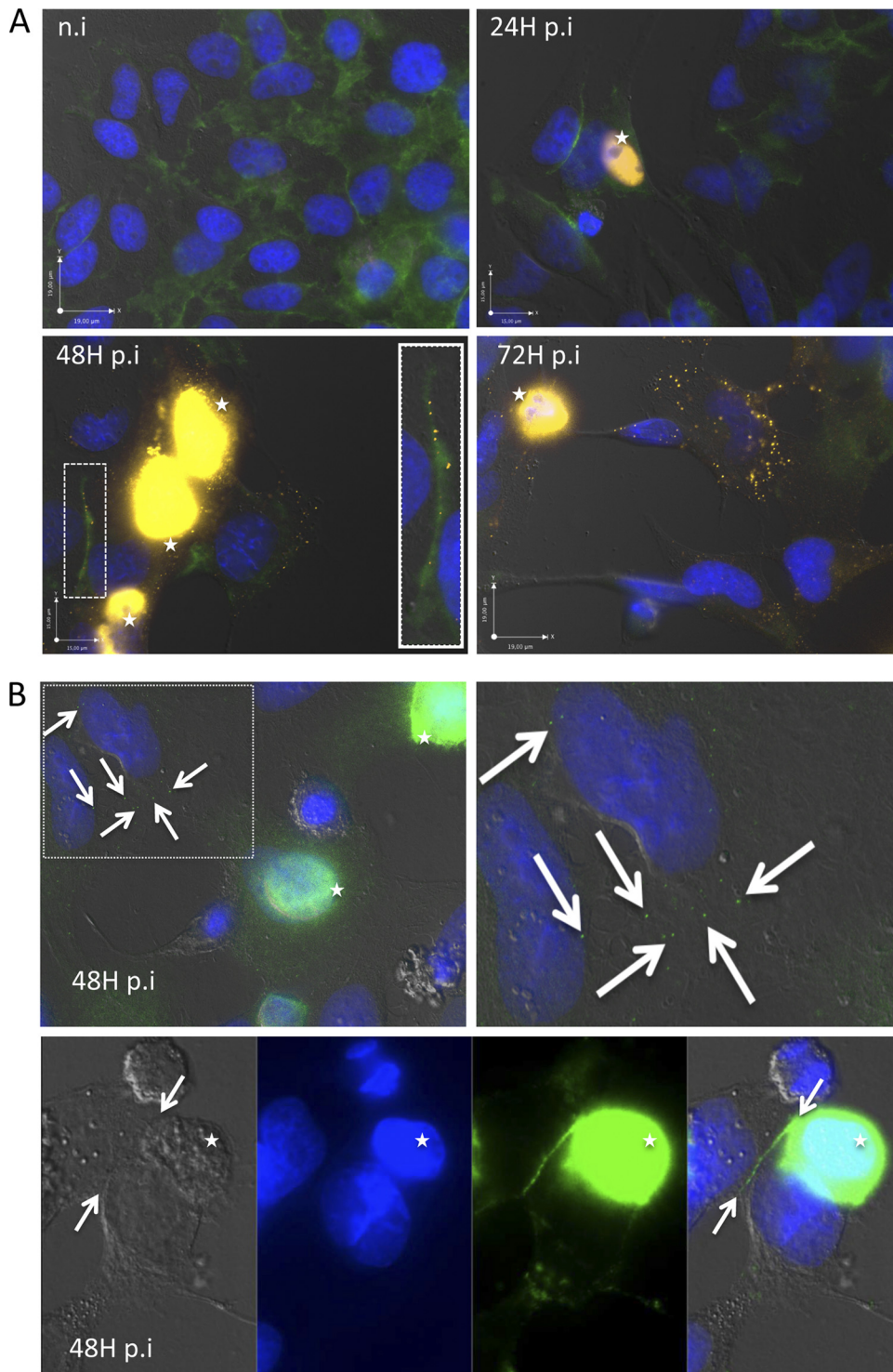


**FIG 1** Escape of penton dodecahedron (Pt-Dd) from Ad3-infected cells. (A) HeLa cells were infected with 0.1 PFU/cell wild-type Ad3 for 24, 48, or 72 h, fixed with 10% formalin, and permeabilized with 0.1% Triton X-100. Cells were stained for DSG-2 expression using rabbit polyclonal anti-DSG-2 (GeneTex) and fluorescein isothiocyanate (FITC)-labeled anti-rabbit secondary antibodies (Jackson ImmunoResearch). Dodecahedra were localized using mouse monoclonal anti-fiber antibodies (Abcam, United Kingdom) and Cy3-labeled anti-mouse secondary antibodies (Jackson ImmunoResearch). Cell nuclei were stained using DAPI (4',6-diamidino-2-phenylindole) (in blue). A close-up view at 48 hpi (white rectangle) shows orange dots along the DSG-2 signal at the contact between two cells. Infected cells are indicated by white stars. n.i., not infected. (B) HeLa cells were infected with wild-type Ad3, fixed, and permeabilized as described above. Dodecahedra were then identified using rabbit polyclonal anti-Pt-Dd (2) and FITC-labeled anti-rabbit secondary antibodies. Pt-Dd staining in noninfected cells is denoted by white arrows. In the lower panel, Pt-Dd staining was observed at the interface between two adjacent cells. Cells were observed using an Olympus IX81 microscope.

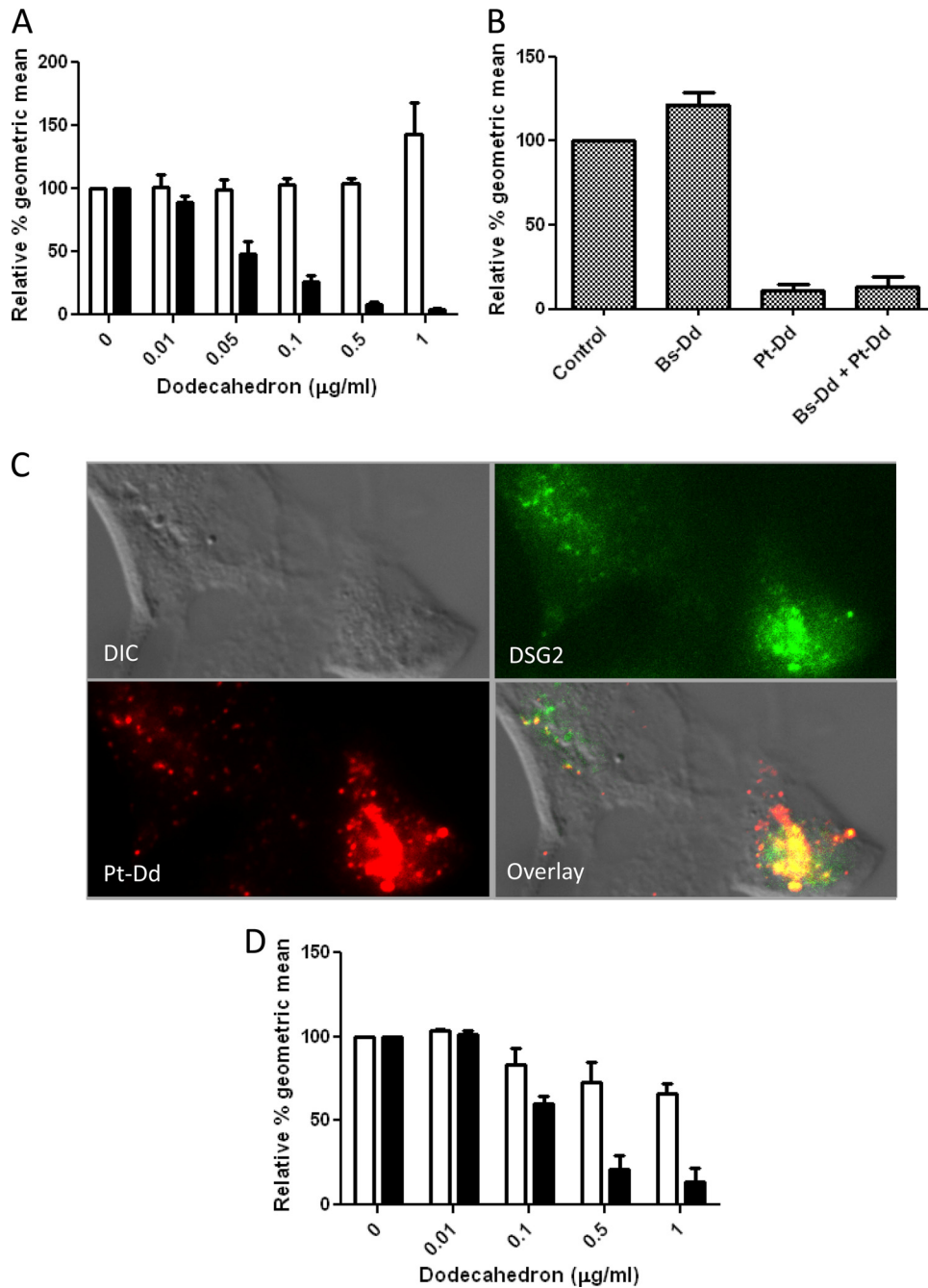


**FIG 2** Pt-Dd interactions with the Ad3 attachment molecule desmoglein-2. (A) To assess competition between dodecahedra and Ad3-EGFP, Bs-Dd or Pt-Dd was added to A549 cells for 30 min at room temperature prior to transduction with replication-deficient Ad3-EGFP at 1 fluorescent forming unit (FFU)/cell. Twenty-four hours later, EGFP expression was analyzed by flow cytometry. Relative geometric means are derived from EGFP expression in the absence of Dd (100%). White bars represent data from Bs-Dd-treated cells, and black bars represent data from Pt-Dd-treated cells. (B) Dodecahedra (1 µg) were added to A549 cells and incubated at 37°C for 2 h. Cells were then washed twice with phosphate-buffered saline (PBS), and Ad3-EGFP was added in serum-free Dulbecco's modified Eagle medium (DMEM) at 1 FFU/cell. Following an additional 2-h incubation at 37°C, cells were washed twice using PBS, and 2 ml of DMEM supplemented with 10% fetal bovine serum (FBS) was added. Cells were incubated overnight at 37°C, and EGFP expression was determined by flow cytometry. (C) To monitor DSG-2 internalization with Pt-Dd, A549 cells were incubated at 37°C for 2 h with Cy5-Pt-Dd (red signal) in DMEM. Cells were fixed, permeabilized, and incubated for 1 h at room temperature with a 1:250 dilution of rabbit anti-DSG-2 antibody (GeneTex Inc.). After PBS washes, cells were incubated for 30 min at room temperature with a 1:250 dilution of FITC anti-rabbit immunoglobulins (Jackson ImmunoResearch) (green signal). DIC, differential interference contrast. (D) Dodecahedra were added to primary human endothelial cells (HUVEC) for 30 min at room temperature prior to transduction with Ad3-EGFP (1 FFU/cell). Twenty-four hours later, EGFP expression was detected by flow cytometry. Relative geometric means are derived from EGFP expression in the absence of Dd (100%). White bars represent data from Bs-Dd-treated cells, and black bars represent data from Pt-Dd-treated cells.

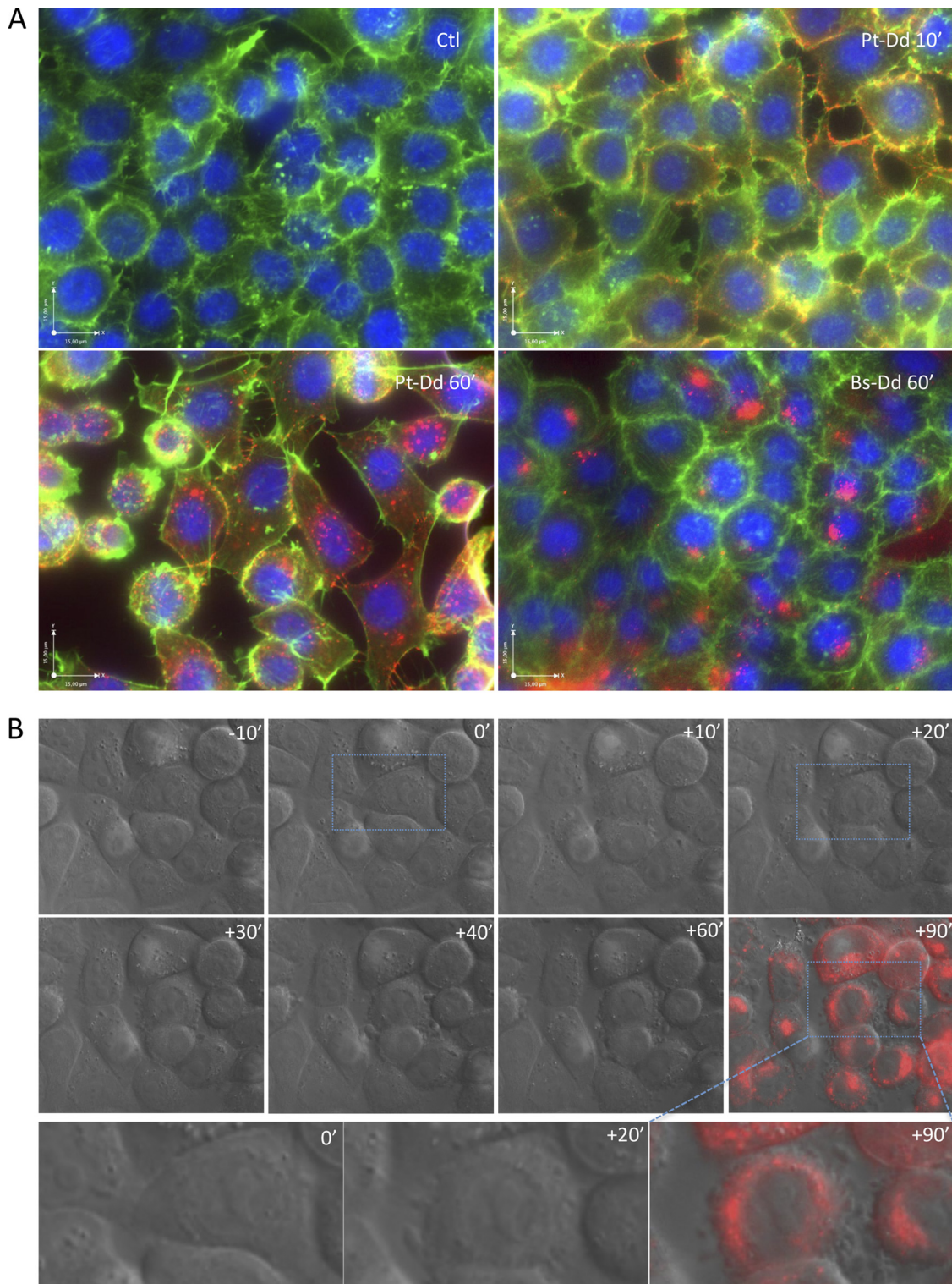


**FIG 3** Remodeling of cellular morphology by Pt-Dd. (A) HeLa cells were grown on glass coverslips and incubated with either Cy5–Bs-Dd or Cy5–Pt-Dd (red signal) at 37°C for the indicated time. Cells were fixed, permeabilized, and incubated for 30 min at room temperature with rhodamine-conjugated phalloidin (Sigma) (pseudocolored in green). Nuclei were stained using Vectashield mounting medium with DAPI (Vector Laboratories) (blue signal). Cells were observed using an Olympus IX81 microscope. Ctl, control. (B) HeLa cells were grown in glass chambers (Mattek) and observed in the DIC channel for 10 min before the addition of Cy5–Pt-Dd and then for an additional 120 min after Cy5–Pt-Dd addition, at a rate of 3 frames per minute. After 60 min, Cy5–Pt-Dd was withdrawn and replaced with prewarmed medium to allow monitoring in the Cy5 channel (red signal). The images shown were extracted from Movie S1 in the supplemental material at the indicated time before or after Pt-Dd addition. The lower panel shows an enlarged view of the image delineated by blue squares in the upper panel. Observation was performed on a thermostatic Olympus IX81 microscope.

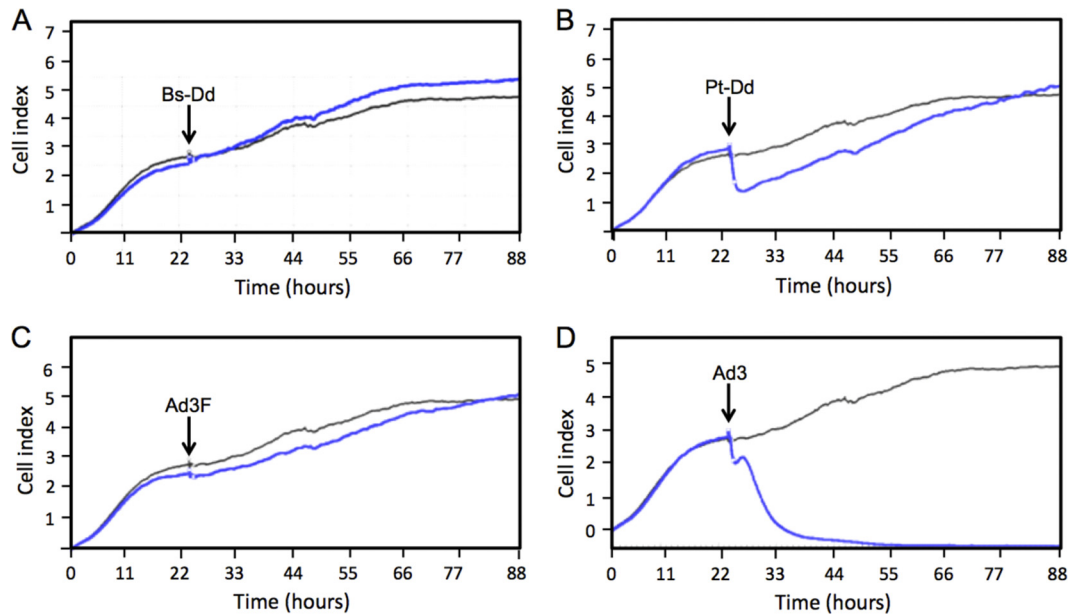


**FIG 4** Cell remodeling depends on the presence of Ad3 fiber in a virus or virus-like context. A549 cells were cultured in DMEM supplemented with 10% FBS in E-plates (ACEA Biosciences, San Diego, CA) which carried microelectronic cell sensor arrays. After 24 h, 0.1  $\mu$ g of Bs-Dd (A), Pt-Dd (B), recombinant trimeric Ad3 fiber (Ad3F) (6) (C), or wild-type Ad3 (D) was added directly to the wells (indicated by black arrows), and the electrical properties of the sensor were measured over the following 64 h using the xCELLigence system (Roche Diagnostics, Burgess Hill, United Kingdom) and are represented by blue lines in each of the graphs. Sensor properties of control cells, to which no proteins were added, are indicated by the gray lines in each graph.

min led to its intracellular localization and disruption of the monolayer, as well as cell rounding (Fig. 3A). In contrast, Bs-Dd was internalized, but no cell remodeling or disruption of the monolayer was detected.

This effect was reproduced using live cell imaging of Cy5-labeled Pt-Dd added to cell monolayers. Movie S1 in the supplemental material and Fig. 3B show that cells tended to retract as soon as 20 min following Cy5–Pt-Dd addition. This observation is in agreement with previous observations of an epithelial-to-mesenchymal transition (EMT) triggered by Pt-Dd (13). These cellular changes were not found in the presence of Bs-Dd (data not shown).

To define the adenovirus protein involved in cell remodeling, a real-time cell analyzer was used to monitor biological changes in A549 cells. Cells were cultured and monitored in E-plates for 24 h prior to the addition of Bs-Dd, Pt-Dd, recombinant Ad3 fiber trimers (6), or wild-type Ad3. These plates carry microelectronic cell sensor arrays, allowing the number of cells as well as the viability, morphology, and degree of adhesion of the cells within each well to be monitored through changes in electrical impedance. Changes across the sensor surface were detected in response to the addition of Pt-Dd (Fig. 4B, blue line) but not following the addition of Bs-Dd (Fig. 4A, blue line), suggesting that Pt-Dd may have affected the morphology of the cells on the electrode and/or the degree of adhesion of these cells to the sensor surface. This supports the data obtained by microscopy (Fig. 3A and B; see also Movie S1 in the supplemental material). The addition of Ad3 to the A549 monolayer initially caused similar changes in electrical impedance in the hours immediately after the addition of the virus (Fig. 4D, blue line). However, in the presence of wild-type virus, the cell index did not recover since virus replication led to cytopathic effect and detachment of all cells. Interestingly, recombinant trimeric fiber

knob purified from *Escherichia coli* did not mimic these cellular effects (Fig. 4C, blue line) despite its interaction with DSG-2. This suggests that the fiber must be present in a virus or virus-like particle (the dodecahedron) to effect cellular changes.

The data presented in this study suggest a biological function for the large excess of fiber and penton base proteins which are produced and assembled into dodecahedra during the Ad3 infectious cycle (1). Pt-Dd interacts with intercellular junctions (Fig. 1), competes with Ad3 for cell entry (Fig. 2), and triggers cell remodeling (Fig. 3 and 4; see also Movie S1 in the supplemental material). In the future, we aim to develop these findings and address the functional relevance of Pt-Dd *in vivo*. It has previously been shown that excess penton base proteins are released from Ad2-infected cells, and it was suggested that this may be to aid in the dissemination of this virus (10). In this study, a similar release of Ad3 proteins was observed, but in addition to the simple blocking of receptors, Ad3 dodecahedra induced changes in cell morphology, suggesting a specific function of this complex in supporting the spread of virus. Interestingly, a previous study has shown that Ad5 fiber remodels polarized epithelial cells to aid in the dissemination of Ad5 (5, 12). Therefore, we hypothesize that the shape of this unusual virus-like particle, as well as its overproduction during the virus replication cycle, may have evolved to assist the spread of progeny virions in three dimensions from the initial point of infection by destroying cell-tissue cohesion and also, by internalizing cell surface DSG-2 molecules, prevents direct capture of Ad3 by surrounding cells (see Fig. S3 in the supplemental material).

#### ACKNOWLEDGMENTS

We thank Daphna Fenel and Christine Moriscot from the electron microscopy platform as well as Françoise Lacroix and Jean Philippe Kleman

from the photonic platform for support and access to instruments. We are indebted to Natalie Fox for her advice and encouragement.

This work is supported by the “Fond d’intervention, Université Joseph Fourier de Grenoble” and Yorkshire Cancer Research.

## REFERENCES

1. Fender P, Boussaid A, Mezin P, Chroboczek J. 2005. Synthesis, cellular localization, and quantification of penton-dodecahedron in serotype 3 adenovirus-infected cells. *Virology* 340:167–173.
2. Fender P, Ruigrok RW, Gout E, Buffet S, Chroboczek J. 1997. Adenovirus dodecahedron, a new vector for human gene transfer. *Nat. Biotechnol.* 15:52–56.
3. Fuschiotti P, et al. 2006. Structure of the dodecahedral penton particle from human adenovirus type 3. *J. Mol. Biol.* 356:510–520.
4. Garcel A, Gout E, Timmins J, Chroboczek J, Fender P. 2006. Protein transduction into human cells by adenovirus dodecahedron using WW domains as universal adaptors. *J. Gene Med.* 8:524–531.
5. Greber UF. 2002. Signalling in viral entry. *Cell. Mol. Life Sci.* 59:608–626.
6. Hall K, Blair Zajdel ME, Blair GE. 2009. Defining the role of CD46, CD80 and CD86 in mediating adenovirus type 3 fiber interactions with host cells. *Virology* 392:222–229.
7. Roelvink PW, et al. 1998. The coxsackievirus-adenovirus receptor protein can function as a cellular attachment protein for adenovirus serotypes from subgroups A, C, D, E, and F. *J. Virol.* 72:7909–7915.
8. Schoehn G, Fender P, Chroboczek J, Hewat EA. 1996. Adenovirus 3 penton dodecahedron exhibits structural changes of the base on fibre binding. *EMBO J.* 15:6841–6846.
9. Sirena D, Ruzsics Z, Schaffner W, Greber UF, Hemmi S. 2005. The nucleotide sequence and a first generation gene transfer vector of species B human adenovirus serotype 3. *Virology* 343:283–298.
10. Trotman LC, Achermann DP, Keller S, Straub M, Greber UF. 2003. Non-classical export of an adenovirus structural protein. *Traffic* 4:390–402.
11. Vives RR, Lortat-Jacob H, Chroboczek J, Fender P. 2004. Heparan sulfate proteoglycan mediates the selective attachment and internalization of serotype 3 human adenovirus dodecahedron. *Virology* 321:332–340.
12. Walters RW, et al. 2002. Adenovirus fiber disrupts CAR-mediated intercellular adhesion allowing virus escape. *Cell* 110:789–799.
13. Wang H, et al. 2011. Desmoglein 2 is a receptor for adenovirus serotypes 3, 7, 11 and 14. *Nat. Med.* 17:96–104.